International Geology Review, Vol. 50, 2008, p. 763–779. DOI: 10.2747/0020-6814.50.8.763

K-Ar Ages and Geochemical + Sr-Nd Isotopic Compositions of Adakitic Volcanic Rocks, Western Shandong Province, Eastern China: Foundering of the Lower Continental Crust

SHEN LIU,[1]

State Key Laboratory of Geological Processes and Mineral Resources, China University of Geosciences, Wuhan 430074, China and State Key Laboratory of Ore Deposit Geochemistry, Institute of Geochemistry, Chinese Academy of Sciences, Guiyang 550002, China

RUI-ZHONG HU,

State Key Laboratory of Ore Deposit Geochemistry, Institute of Geochemistry, Chinese Academy of Sciences, Guiyang 550002, China

SHAN GAO,

State Key Laboratory of Geological Processes and Mineral Resources, China University of Geosciences, Wuhan 430074, China

CAI-XIA FENG, HONG ZHONG, YOUQIANG QI, TAO WANG, LIANG QI, AND GUANGYING FENG

State Key Laboratory of Ore Deposit Geochemistry, Institute of Geochemistry, Chinese Academy of Sciences, Guiyang 550002, China

Abstract

K-Ar age, geochemical, and Sr-Nd isotopic data are reported for western Shandong volcanic rocks with the objectives of deciphering the origin and dynamic significance of Mesozoic magmatic events within the North China craton. K-Ar ages indicate eruption of the volcanic rocks between 116.2 ± 1.1 and 120.3 ± 1.1 Ma. The studied rocks include andesite and dacite that have SiO_2 contents ranging from 59.3 to 65.9 wt% and Al_2O_3 contents from 15.3 to 16.8 wt%; K_2O and Na_2O contents range from 3.4 to 5.1 wt% and 3.1 to 3.8 wt%, respectively, indicating that they belong to the K-rich series. These rocks are depleted in heavy rare-earth elements (HREE) and variably enriched in light rare-earth elements (LREE). They have positive Ba, Sr, and K and negative Nb, Ta, and Ti anomalies. The rocks have high Sr ranging from 492 to 1665 ppm and relatively low Yb (0.77–1.75 ppm) and Y contents (9.5–17.1 ppm), resulting in high Sr/Y (52–102) and La/Yb ratios (28–45), characteristic of adakites. εNd(t) and initial Sr isotopic compositions range from –13.2 to –10.3 and from 0.7089 to 0.7098, respectively. These geochemical features are consistent with an origin from adakitic magmas that were likely derived from dehydration melting of a delaminated lower crust. The relatively high MgO, Cr, and Ni contents in the analyzed rocks suggest that interaction between melts and peridotite may have occurred before eruption. This study provides further evidence for foundering of lower crust accompanied by lithosphere thinning beneath the North China craton (NCC).

Introduction

DEFANT AND DRUMMOND (1990) first used the term "adakite" to describe subduction-related intermediate to acidic volcanic and plutonic rocks with distinct geochemical characteristics, such as high, Al, Na, and Sr contents, high Sr/Y and La/Yb ratios, and low Y and Yb contents, suggesting an origin by partial melting of hydrated mafic source rocks in the form of eclogite or garnet amphibolite (Rapp et al., 1991; Martin, 1998). Due to their contribution to the understanding of crust-mantle interactions and geodynamic regimes, attention has been drawn toward adakitic rocks, and five models for adakite generation have been proposed: (1) melting of subducted oceanic crust (Defant and Drummond, 1990; Martin, 1998), followed by interaction with the overlying mantle wedge (Kay, 1978); (2) melting of mantle peridotite under hydrous conditions (Stern and Hanson, 1991); (3) melting of thickened mafic lower

[1]Corresponding author; email: liushen@vip.gyig.ac.cn

continental crust (Atherton and Petford, 1993); (4) melting of delaminated continental lower crust (Atherton and Petford, 1993; Xu et al., 2002); and (5) assimilation-fractional crystallization (AFC) processes (e.g., Castillo et al., 1999; Macpherson et al., 2006).

Foundering of continental lower crust into underlying, convecting mantle has been proposed as one means to explain the unusually evolved chemical composition of the Earth's continental crust (Kay and Kay, 1991; Rudnick, 1995). The eastern NCC is perhaps the best example of an Archean craton that lost its lithospheric keel (Fig. 1A) (Menizes et al., 1993; Griffin et al., 1998; Gao et al., 2002), and thus is an ideal place to evaluate the hypothesis of lower crust foundering. This process has been confirmed within the North China craton based on the study of high-Mg andesites, dacites, and adakitic volcanic rocks (Gao et al., 2004) and the Sulu belt (Guo et al., 2006). Nevertheless, direct evidence of this process is still relatively scarce in the interior of the NCC. In this study, we report a new adakite locality from western Shandong Province (Fig. 1B) and present new geochemical and isotopic data to further prove the foundering of mafic lower continental crust within the NCC.

Geological Background and Petrology

The eastern portion of the NCC in Shandong Province is divided into two parts by the Tanlu fault, Jiaodong to the east and Luxi to the west (Fig. 1B). Mesozoic intrusive and volcanic rocks are widely exposed in the Luxi area. Previous studies indicate that magmatic activities mainly took place in Luxi between the Late Jurassic and Early Cretaceous (144–115 Ma) (Xu et al., 1993; Tan and Lin, 1994; Qiu et al., 2001; Zhang and Sun, 2002; Guo et al., 2003; Liu et al., 2004; unpubl. data; Xu et al., 2004a, 2004b, 2004c; Zhang et al., 2004, 2005a). In addition, it was suggested that the magmas were derived from re-enriched lithospheric mantle.

The study area is located in southeastern Luxi, adjacent to Fangcheng (Fig. 1B). The adakitic rocks occur as small lava flows in a graben within the continental basin; their exposures are controlled by the E-W–striking fault and cover an area of ~1.5 km^2. No basaltic rocks are associated with the adakitic rocks, but Fangcheng basalts have been discovered in the southeast part of the study area (Zhang et al., 2002). The volcanic formation consists of microporphyritic adakitic andesite and dacite (Fig. 2A); the lavas are interlatyered with tuffaceous conglomerate and andesitic breccia.

The andesite contains abundant (25–40%) phenocrysts of plagioclase and pyroxene (0.3–1.5 mm). Minor phenocrysts of amphibole and biotite are also present (Fig. 2). The groundmass is composed of fine-grained (0.03–0.06 mm) plagioclase and minor magnetite. The dacite consists of 35% coarse-grained (0.5–2.0 mm) phenocrysts of plagioclase, quartz, and minor amphibole and biotite, together with a 60% matrix of fine-grained (0.03–0.05 mm) plagioclase, quartz, and magnetite (Fig. 2).

Analytical Techniques

The weathered surfaces of the samples were removed. The samples were then cut, cleared with deionized water, and crushed in an agate mill. The pulverized samples were used for K–Ar geochronological, major and trace element, and Sr–Nd isotopic analyses. Potassium-argon geochronology was performed using the MM-1200 spectrometer at the Institute of Geology, China Seismological Bureau. Major oxides were analyzed by a Phillips PW4400 sequential X-ray fluorescence spectrometer at the Institute of Geochemistry, Chinese Academy of Sciences. Analytical precision for the major oxides was estimated to be better than 5%. Loss on ignition was obtained from 1 g powder after calcinations at 950°C for 3 hours. The results are listed in Table 1. Trace elements were analyzed with a POEMS ICP-MS at the National Research Center of Geoanalysis, Chinese Academy of Geosciences, following procedures described by Qi et al. (2000). The discrepancy between triplicates analyses of the same samples is less than 5% for all the analyzed elements (Table 1).

For Rb-Sr and Sm-Nd isotopic analyses, the samples were spiked with mixed isotope tracers, dissolved in Teflon capsules with HF+ HNO_3 acids, and separated by conventional cation-exchange technique. Isotopic ratios were measured on the MAT-262 mass spectrometer at the Institute of Geology and Geophysics, Chinese Academy of Sciences (IGGCAS). Procedural blanks were <100 pg for Sm and Nd and <500 pg for Rb and Sr. The $^{143}Nd/^{144}Nd$ ratios were corrected for mass fractionation by normalization to $^{146}Nd/^{144}Nd = 0.7219$ and $^{87}Sr/^{86}Sr$ ratios to $^{86}Sr/^{88}Sr = 0.1194$. The measured Sr and Nd isotope standard values are $^{87}Sr/^{86}Sr = 0.710245 \pm 14$ (2σ) for NBS987 and $^{143}Nd/^{144}Nd = 0.512150 \pm 9$ (2σ) for AMES. The results are listed in Table 2.

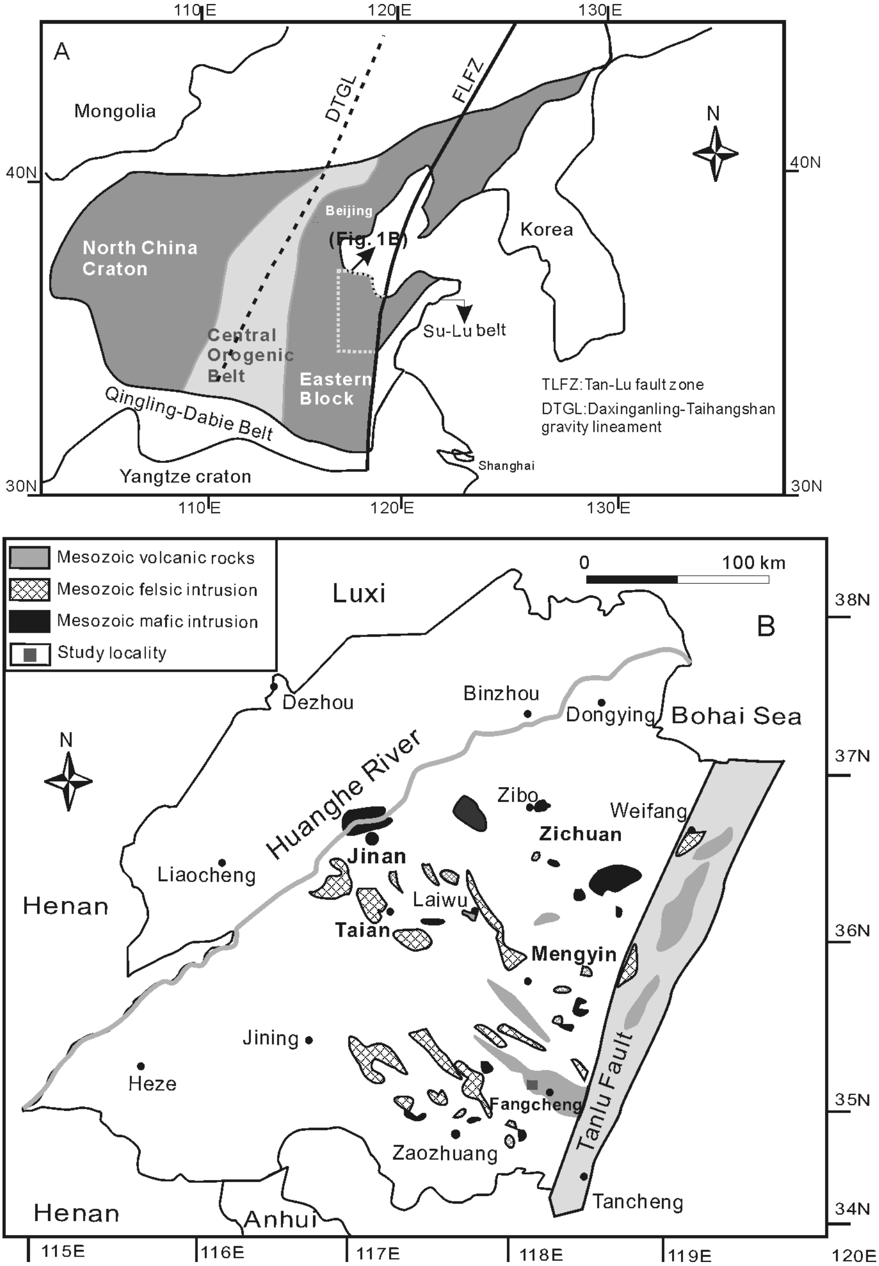

FIG. 1. A. Simplified teconic map of eastern China (modified after Xu, 2002). B. Geologic sketch map of Luxi in Shandong Province. Inset shows sampling location of the adakitic lavas.

Results

K-Ar ages

Field relationships indicate that the volcanic rocks erupted after the Early Cretaceous (Fig. 1B).

The andesite and dacite give 116.2 ± 1.1 Ma and 120.3 ± 1.1 Ma K–Ar ages, respectively (Table 1), which are interpreted to be the eruption ages.

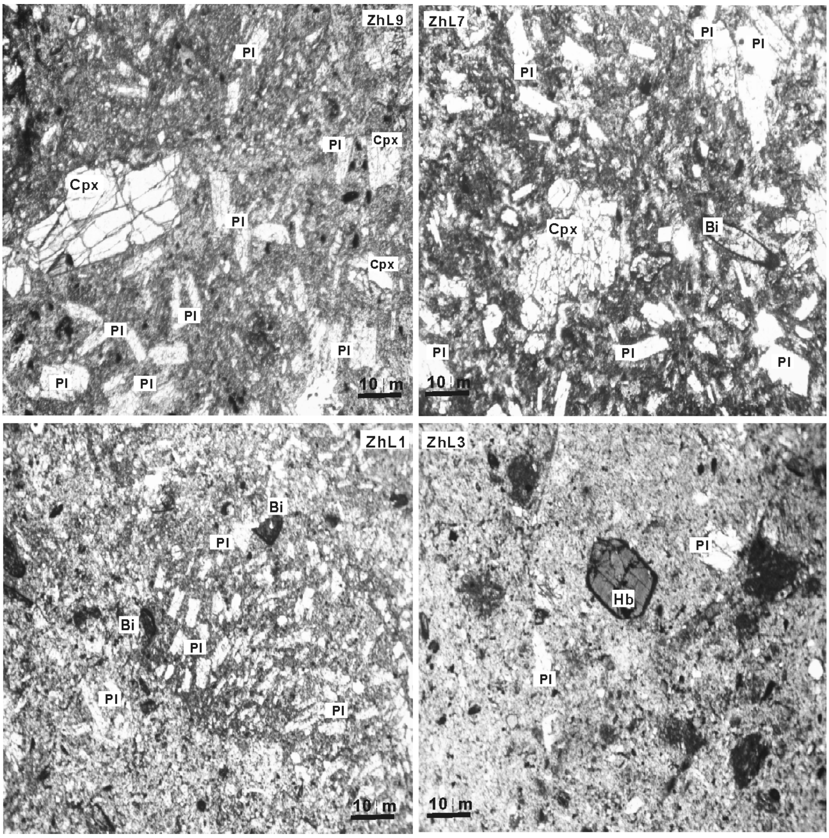

FIG. 2. Photomicrographs showing petrographic features of the volcanic rocks in Luxi. Abbreviations: Cpx = clinopyroxene, Pl = plagioclase, Hb = amphibole, Bi = biotite.

TABLE 1. K-Ar Ages on Whole-Rock Powders[1]

Sample	Dating method	K(%)	^{40}Ar rad (mol/g)	^{40}Ar rad (%)	Ages (±1σ, Ma)
ZhL3	Whole rock (K-Ar)	2.98	5.87E-10	94.10	116.2±1.1
ZhL6	Whole rock (K-Ar)	3.96	8.55E-10	97.16	120.3±1.1

[1]Parameters for ^{40}K: $M_e = 0.581 \times 10^{-10}$ year^{-1}; $M_\beta = 4.962 \times 10^{-10}$ year^{-1}; ^{40}K = 0.01167 atom% (Steiger and Jäger, 1977).

Major and trace elements

The adakites have high SiO_2 (59–66 wt%), Al_2O_3 (15.3–16.8 wt%), Sr (492–1665 ppm), and Ba (1004–1620 ppm) contents, low Yb (0.77–1.75 ppm) and Y contents (9.5–17.1 ppm), as well as elevated Sr/Y (52–102) and La/Yb (28–45) ratios (Figs. 3 and 4), similar to those of typical adakites (Defant and Drummond, 1990) except that they have high K contents (K_2O = 3.4–5.1 wt% and $K_2O>Na_2O$). Furthermore, the adakites exhibit relatively high MgO (1.1–3.5 wt%) and Mg$^{\#}$ (36–52), Cr (56–195 ppm), Ni (25–86 ppm), and Th contents (4.9–8.5 ppm) and low Th/Ce ratios (Table 2; Figs. 5B and 5D–5F). These compositional features are thought to be

TABLE 2. Major Oxides (wt%) and Trace Elements (ppm) of Volcanic Rocks from Luxi, Southeastern North China Craton[1]

Sample:	ZhL1	ZhL2	ZhL3	ZhL4	ZhL5	ZhL6	ZhL7	ZhL9	ZhL10	ZhL11
Rock type:	Dacite	Andesite	Dacite	Andesite	Andesite	Andesite	Andesite	Andesite	Andesite	Andesite
SiO_2	65.89	62.50	65.54	61.96	61.33	59.33	60.81	60.68	59.54	59.42
TiO2	0.55	0.71	0.46	0.70	0.95	1.17	0.86	0.80	1.23	0.86
Al_2O_3	16.37	15.93	16.47	15.82	16.31	15.5	15.39	15.26	16.77	15.55
Fe_2O_3	4.04	5.46	4.98	5.39	6.03	7.21	6.89	6.19	5.48	5.54
MnO	0.07	0.09	0.11	0.12	0.10	0.14	0.08	0.16	0.13	0.06
MgO	1.13	1.61	1.31	1.79	2.13	3.53	2.50	2.57	2.34	2.98
CaO	1.32	3.42	2.76	3.23	4.14	4.43	3.94	4.77	5.79	5.33
Na_2O	3.81	3.76	3.47	3.68	3.38	3.18	3.08	3.57	3.26	3.54
K_2O	4.80	4.72	3.44	5.03	3.49	3.82	4.45	3.82	3.71	3.35
P_2O_5	0.21	0.34	0.22	0.35	0.43	0.55	0.34	0.44	0.48	0.44
LOI	1.67	1.08	0.83	1.46	1.69	1.40	1.23	1.66	0.96	2.72
Total	99.86	99.63	99.59	99.52	99.97	100.26	99.56	99.93	99.69	99.80
Mg#	35.6	36.9	39.5	39.7	41.2	49.2	41.8	45.1	41.7	51.6
Sc	11.4	11.6	9.0	12.1	13.3	14.4	14.9	13.7	14.7	12.1
Cs	2.25	1.20	2.46	1.53	0.46	0.56	0.39	1.65	0.55	0.19
Cr	96.1	56.9	68.7	66.4	78.8	68.8	161	195	66.7	192
Co	14.1	14.3	8.3	15.3	14.7	21.2	18.3	19.7	18.8	18.4
Ni	48.1	27.0	24.8	31.8	39.3	47.8	43.7	85.9	48.5	81.1
Cu	24.3	21.0	17.3	32.4	26.1	29.5	26.4	25.5	30.4	43.6
Zn	58.2	84.5	49.8	67.8	104	97.0	71.9	81.2	87.1	59.6
Ga	20.2	19.4	17.8	19.5	20.9	22.1	19.4	20.0	22.9	19.0
Ba	1620	1336	1274	1423	1089	1004	1285	1407	1029	1367
Rb	151	132	105	144	74.9	85.9	68.0	136	82.5	112
Sr	492	884	915	876	1080	1603	894	988	1665	1224
Y	9.5	12.8	9.8	12.6	17.0	15.7	14.2	14.9	17.1	14.6
Zr	188	222	141	219	229	238	198	258	251	216
Hf	4.30	4.87	3.46	4.75	5.51	5.88	4.60	5.62	6.09	4.74
Nb	6.5	9.3	5.3	9.2	10.1	16.8	8.9	11.7	17.8	10.4
Ta	0.36	0.49	0.31	0.50	0.46	0.86	0.49	0.56	0.93	0.53
Th	6.62	8.11	4.94	8.15	7.16	7.38	7.04	8.51	7.89	6.81
U	1.48	1.62	1.55	1.65	1.83	1.21	1.96	1.77	1.60	1.30
Pb	27.8	20.5	30.2	20.4	14.0	9.40	21.4	19.4	9.20	18.4
La	46.0	58.3	35.1	57.9	88.2	61.7	72.9	79.6	73.8	71.1
Ce	75.4	105	61.6	105	117	115	98.4	142	121	108
Pr	8.78	12.1	7.04	11.8	17.8	14.1	15.1	19.0	16.5	13.1
Nd	32.0	44.9	27.3	43.8	69.5	55.5	58.4	73.7	65.9	50.3
Sm	4.64	6.50	3.99	6.35	10.4	8.18	8.98	10.5	9.73	7.45
Eu	1.33	1.78	1.16	1.71	2.73	2.32	2.30	2.74	2.74	2.02
Gd	3.33	4.39	2.95	4.48	7.45	5.94	6.44	7.56	7.25	5.28
Tb	0.42	0.57	0.37	0.56	0.97	0.76	0.87	0.91	0.94	0.63
Dy	2.03	2.76	1.91	2.69	4.73	3.86	4.34	4.42	4.66	3.13
Ho	0.34	0.48	0.34	0.48	0.81	0.65	0.74	0.73	0.80	0.53
Er	0.91	1.34	0.94	1.31	2.17	1.83	2.07	1.95	2.16	1.40
Tm	0.12	0.16	0.12	0.17	0.26	0.23	0.26	0.23	0.27	0.17
Yb	0.77	1.19	0.81	1.14	1.36	1.49	1.70	1.21	1.75	1.12
Lu	0.11	0.17	0.12	0.16	0.24	0.21	0.26	0.21	0.26	0.16
Eu/Eu*	1.03	1.02	1.03	0.98	0.95	1.02	0.93	0.94	1.00	0.99
Sr/Y	51.5	69.2	93.5	69.5	63.6	102	62.9	66.3	97.3	84.1
(La/Yb)N	40.5	33.1	29.2	34.2	43.8	28.0	29.0	44.5	28.5	42.9

[1]LOI = loss on ignition; $Mg^{\#} = 100*Mg/(Mg+\Sigma Fe)$ atomic ratio, $Eu/Eu = EuN/(SmN+GdN)^{1/2}$; N = chondrite-normalized.

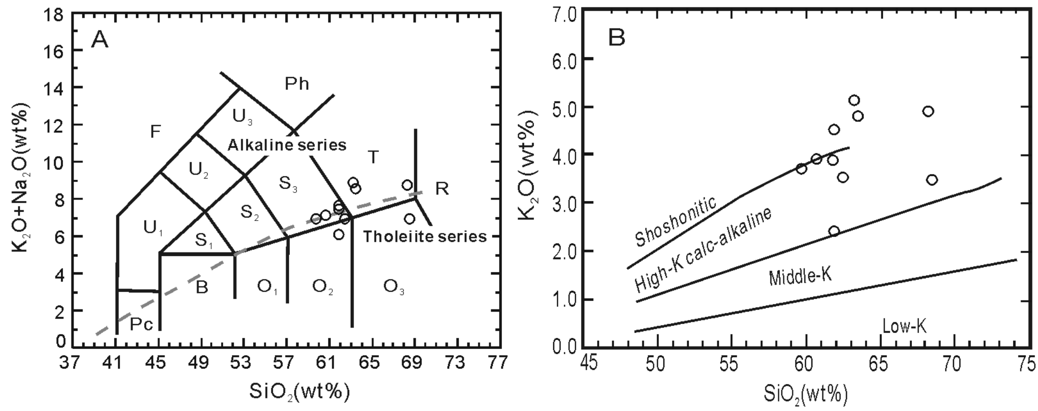

FIG. 3. Chemical classification and identification diagrams of the volcanic rocks in Luxi. A. K_2O + Na_2O vs. SiO_2 (Le Bas et al., 1986). B. K_2O vs SiO_2. Abbreviations: Pc = picrobasalt; B = basalt; O1 = basaltic andesite; O2 = andesite; O3 = dacite; R = rhyolite; S1 = trachybasalt; S2 = basaltic trachyandesite; S3 = trachyandesite; T = trachyte; U1 = basanite; U2 = phonotephrite; U3 = tephriphonolite; Ph = phonolite; F = foidite. The legends for other diagrams are same as Figure 3.

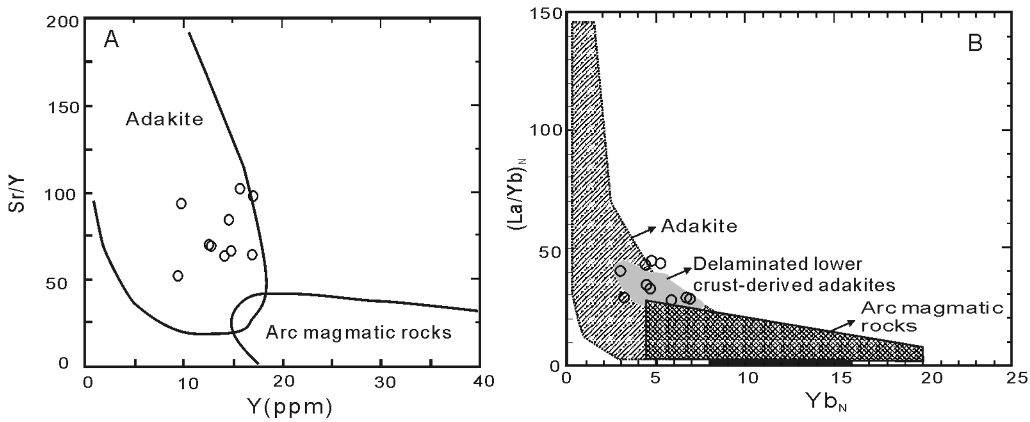

FIG. 4. Sr/Y vs. Y (A) and (La/Yb) N vs. YbN (B) diagrams (Defant and Drummond, 1990) of the high-K adakitic lavas from Luxi, southeastern NCC. Data for delaminated lower crust-derived adakitic rocks are from Xu et al. (2002) and Wang et al. (2004).

derived from melting of subducted oceanic crust or delaminated lower crust (Defant and Drummond, 1990; Kay et al., 1993; Drummond et al., 1996; Stern and Kilian, 1996; Sajona et al., 2000; Defant et al., 2002; Aguillo'n-Robles et al., 2001; Xu et al., 2002; Wang et al., 2004; Martin et al., 2005). The adakitic volcanic rocks display significantly enriched LREE, strongly depleted HREE, and no obvious Eu anomalies in chondrite-normalized REE pattern (Fig. 6A). The samples are also depleted in high-field-strength elements (HFSE), Nb, Ta, and Ti in the N-MORB–normalized trace element spider diagram (Fig. 6B).

Sr-Nd isotopic ratios

The Nd and Sr isotopic compositions of the samples are characterized by high $^{87}Sr/^{86}Sr_i$ (0.709–0.711), low $(^{143}Nd/^{144}Nd)_i$ (0.5118–0.5120) and negative $\varepsilon_{Nd}(t)$ values (–13.2 to –10.3) (Table 3; Fig.7). They fall within the range of the isotopic composition of Jurassic–Cretaceous intermediate-acidic rocks in the eastern Yangtze block (Ningzhen,

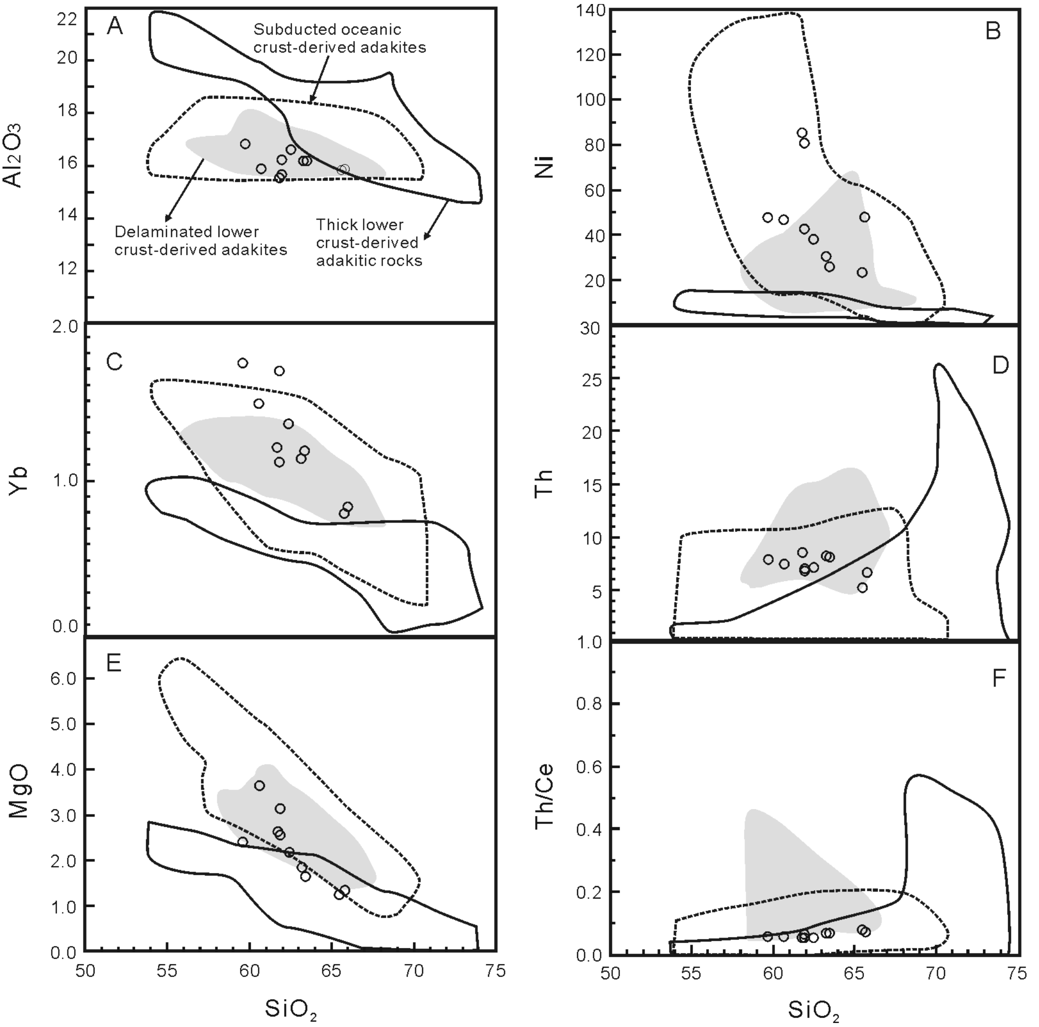

FIG. 5. Variation diagrams for major oxides and trace elements vs. SiO_2 contents for the adakitic rocks. Data for delaminated lower crust–derived adakitic rocks are constructed using the same data sources as Figure 3. Data for subducted oceanic crust-derived adakites are from Defant and Drummond (1990), Kay et al. (1993), Drummond et al. (1996), Stern and Kilian (1996), Sajona et al. (2000), Defant et al. (2002), Aguillo'n-Robles et al. (2001), and Martin et al. (2005). Data for thick lower crust–derived adakitic rocks are from Atherton and Petford (1993), Muir et al. (1995), Petford and Atherton (1996), Johnson et al. (1997), and Xiong et al. (2003).

Yueshan, and Tongshankou) (Fig. 7; Xu et al., 2002; Wang et al., 2003a, 2003b, 2006).

Discussion

Petrogenesis

Genetic models. Geochemical characteristics of the Luxi adakitic volcanic rocks indicate that they were most likely derived from the melting of delaminated continental lower crust or subducted oceanic crust (Fig. 4), although other models seem plausible. First, it is unlikely that they have been derived by partial melting of a subducted oceanic slab because no evidence exists for Triassic subduction in Luxi (Song and Li, 2001). Hence, there was no subducted oceanic slab beneath this region when these K-rich adakitic volcanic rocks were generated at 116–120 Ma. Moreover, if the adakitic lavas formed by partial

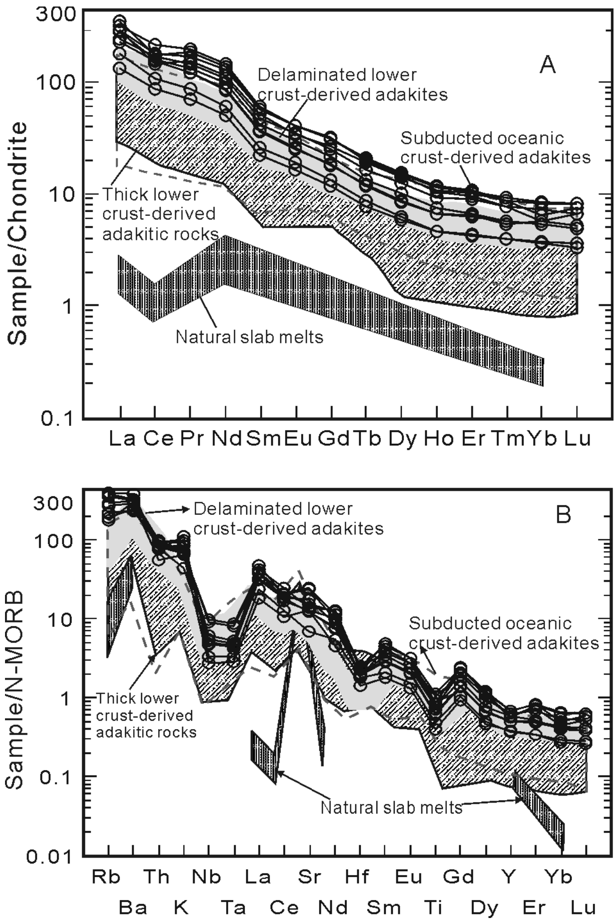

FIG. 6. Chondrite-normalized (A) and N-MORB-normalized spidergrams (B) of Luxi adakitic volcanic rocks, southeastern NCC. Normalized values are after Sun and McDonough (1989). The REE and trace elment data for delaminated lower crust–derived adakitic rocks, subducted oceanic crust–derived adakites, thick lower crust–derived adakites and natural slab melt adakitic rocks are quoted from the same data sources as those in Figure 4. Pure slab melts are after Kepezhinskas et al. (1995).

melting of a subducted oceanic crust, they are supposed to have mid-ocean-ridge basalt (MORB)–like Sr-Nd isotopic compositions, such as those from Cook Island (Stern and Kilian, 1996), Adak Island (Kay, 1978), and Cerro Pampa (Kay et al., 1993; Gao et al., 2004). In contrast, the analyzed adakitic lavas have low $\varepsilon_{Nd}(t)$ (–13.2 to –10.3) and high $(^{87}Sr/^{86}Sr)_i$ (0.709–0.711) isotopic compositions (Table 3; Fig. 7). Thus, partial melting of a subducted oceanic slab was not responsible for the genesis of the adakitic rocks in Luxi.

The Nd-Sr isotopic characteristics (Figs. 7 and 8) and relatively high MgO, Cr, and Ni contents (Fig. 5; Table 1) of the adakitic rocks confirm that a mantle component may have played an important role in their petrogenesis. Our samples exhibit relatively high SO_2 contents (59–66 wt%), ruling out the possibility of magma produced directly by partial melting of hydrous or dry mantle peridotite, because neither can yield melts more silicic than andesite or boninite (Green, 1980; Jahn & Zhang, 1984; Baker et al., 1995). In La/Yb vs La and Ni vs Th plots (Figs. 8A and 8B), the adakitic rocks are more consistent with a partial melting than a fractional crystallization trend. Moreover, no correlations exist between SiO_2 vs. $\varepsilon_{Nd}(t)$ and $(^{87}Sr/^{86}Sr)_i$ (Figs. 9A and

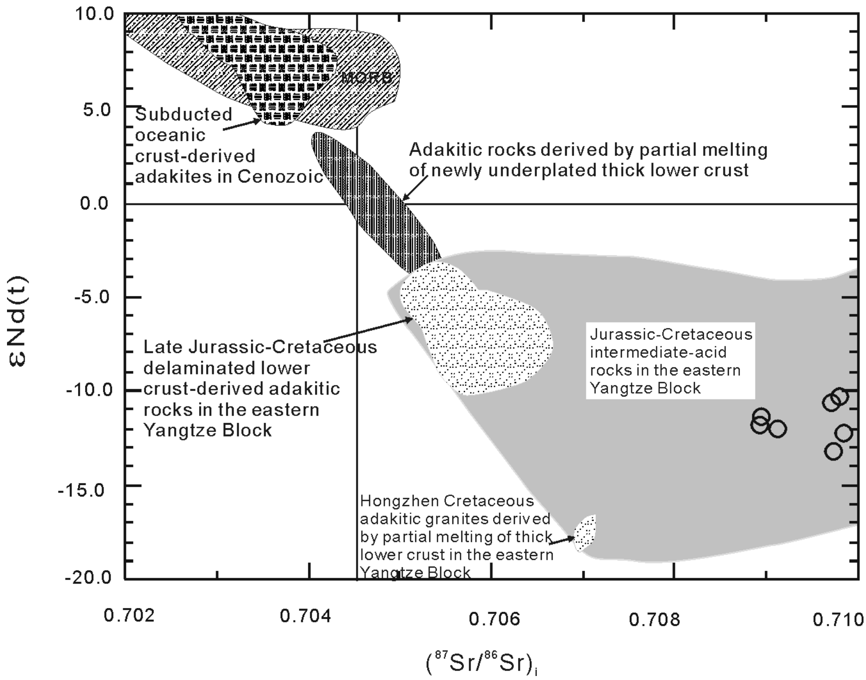

FIG. 7. Nd-Sr isotopic compositions of the adakitic lavas. Data sources are as follows: Luxi adakitic porphyries are from Table 3; adakitic rocks directly derived from a thick crust (lower crustal melting) are after Atherton and Petford (1993), Muir et al. (1995), and Petford and Atherton (1996); Cenozoic subducted oceanic crust–derived adakites are after Defant et al. (1992), Kay et al. (1993), Sajona et al. (2000), and Aguillo'n -Robles et al. (2001); delaminated lower crust–derived adakitic rocks are from Xu et al. (2002) and Wang et al. (2004); the Hongzhen Cretaceous adakitic granites are from Wang et al. (2004); Jurassic–Cretaceous intermediate-acidic rocks in the eastern Yangtze Block are from Wang (2000), Xu et al. (2002), and Wang et al. (2003a, 2003b); MORB are from Mahoney et al. (1998), Xu et al. (2003), Tribuzio et al. (2004), and Xu and Castillo (2004).

TABLE 3. Sr-Nd Isotopic Ratios of Volcanic Rocks from Luxi, Southeastern North China Craton[1]

Sample	$^{147}Sm/^{144}Nd$	$^{143}Nd/^{144}Nd$ (2σ)	$(^{143}Nd/^{144}Nd)_i$	$\varepsilon_{Nd}(t)$	$^{87}Rb/^{86}Sr$	$^{87}Sr/^{86}Sr$(2σ)	$(^{87}Sr/^{86}Sr)_i$
ZhL1	0.0878	0.511885 ± 11	0.511822	–13.2	0.8865	0.711117 ± 13	0.709731
ZhL2	0.0875	0.512025 ± 13	0.511956	–10.3	0.4312	0.710543 ± 13	0.709808
ZhL3	0.0885	0.511936 ± 10	0.511872	–12.2	0.3311	0.71036 ± 13	0.709842
ZhL4	0.0876	0.512009 ± 10	0.511940	–10.6	0.4748	0.710529 ± 12	0.709719
ZhL6	0.0893	0.511946 ± 10	0.511876	–11.9	0.1550	0.709426 ± 13	0.709162
ZhL10	0.0889	0.511976 ± 10	0.511906	–11.3	0.1435	0.709227 ± 12	0.708982
ZhL11	0.0896	0.511947 ± 8	0.511877	–11.8	0.2645	0.709371 ± 13	0.708920

[1]Chondrite Uniform Reservoir (CHUR) values ($^{87}Rb/^{86}Sr$ = 0.0847, $^{87}Sr/^{86}Sr$ = 0.7045, $^{147}Sm/^{144}Nd$ = 0.1967 $^{143}Nd/^{144}Nd$ = 0.512638) are used for the calculation; λRb = 1.42 × 10^{-11} year (Steiger and Jäger, 1977); λSm = 6.54 × 10^{-12} $year^{-1}$ (Lugmair and Harti, 1978).

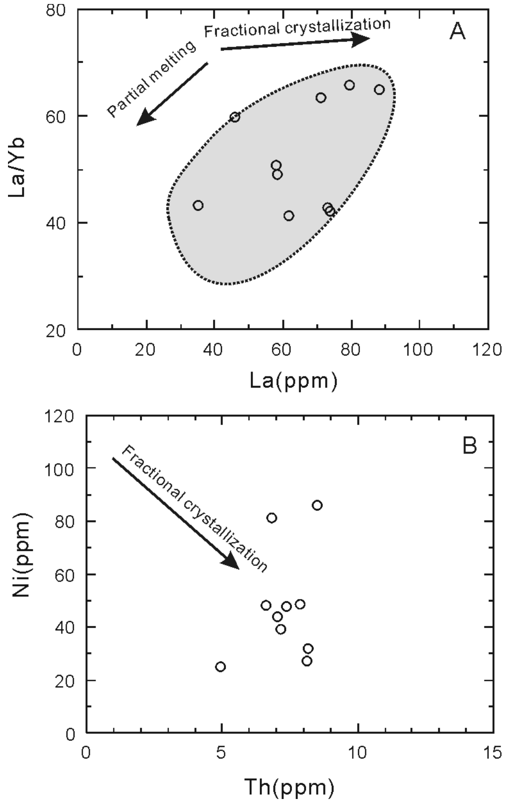

FIG. 8. Plots of La/Yb vs. La (A) and Ni vs Th (B) for the adakitic volcanic rocks from Luxi, southeastern NCC.

9B), clearly indicating that they were probably not generated from an assimilation and fractional crystallization (AFC)–like process; if crustal contamination were extensive, correlations between SiO_2 and Sr and Nd isotopic compositions would be expected. (Castillo et al., 1999). Therefore, lower-crustal melting is thought to be the most likely interpretation for the origin of the adakitic volcanic rocks discussed here.

If the adakitic rocks were derived directly from melting of thickened mafic lower continental crust, they should have relatively low MgO contents and $Mg^{\#}$ values, similar to the experimental melts of Rapp and Watson (1995). However, most samples of the studied adakitic volcanic rocks have relatively high MgO contents and Mg-numbers (Table 2), suggesting that pristine adakitic melts must have interacted to some extent with mantle peridotite.(e.g., Kepezhinskas et al., 1995; Stern and Kilian, 1996; Rapp et al., 1999; Smithies, 2000). In addition, the source of the Luxi adakitic volcanic rocks clearly contains a significant mantle component with depleted Nd isotopic compositions (Table 3; Fig. 7); this is markedly different from those of the lower crust–derived Hongzhen adakitic rocks in the eastern Yangtze block (Fig. 7). Therefore, the most probable scenario that can explain the petrogenesis of the adakitic volcanic rocks in Luxi is partial melting of lower crust during delamination, similar to the model proposed for the Late Jurassic–Cretaceous Ningzhen, Yueshan, and Tongshankou adakitic intrusive rocks in the eastern Yangtze Block (Xu et al., 2002; Wang et al., 2004) and the late Mesozoic adakites in Sulu belt (Guo et al., 2006). Alternatively, the adakitic melts may have interacted with peridotite during their ascent because they have relatively high Mg, Cr, and Ni contents (Kay, 1978; Rapp et al., 1999). This is further attested to by the Pyroxene phenocrysts in the rocks (Fig. 2).

Source nature and genetic mechanism. The western Shandong adakitic rocks show high La/Yb, Sr/Y ratios and low Y and Yb contents (Table 2; Figs. 4 and 6), suggesting that garnet was stable within the source residues when the adakitic magmas were segregated (Defant and Drummond, 1990; Atherton and Petford, 1993; Rapp and Watson, 1995; Drummond et al., 1996; Defant and Kapezhinskas, 2001; Rapp et al., 1999, 2003). Enrichment in Sr (up to 1665 ppm) and absence of significant Eu anomalies (Fig. 6A) indicate plagioclase fractionation was very minor. Generally, Nb tends to reside in amphibole, being at equilibrium with 60–70% SiO_2 melt during partial melting (Pearce and Norry, 1979), whereas Ti partitions into rutile under hydrous mantle conditions (Tatsumi, 1986). However, both elements are depleted in the adakitic rocks (Fig. 6B), which indicates that the source also contained residual rutile and amphibole. An amphibole residue is also consistent with the enriched middle REE patterns of the adakitic rocks (Figs. 6A and 6B) (Wang et al., 2006). Thus, the melting residues were most probably garnet-amphibolites or amphibole-bearing eclogite (Mahoney et al., 1998).

Mesozoic magmatism in the NCC might be related to the Triassic collision and subduction of the Yangtze block (Zhang et al., 2005a) or the subduction of the paleo-Pacific plate (Chen et al., 2004). Volcanic rocks in this study share similar Nd-Sr isotopic characteristics with the Jurassic–Cretaceous intermediate-acidic rocks of the eastern Yangtze block (Fig. 7; Xu et al., 2002; Wang et al., 2003a, 2003b, 2006), suggesting the involvement of

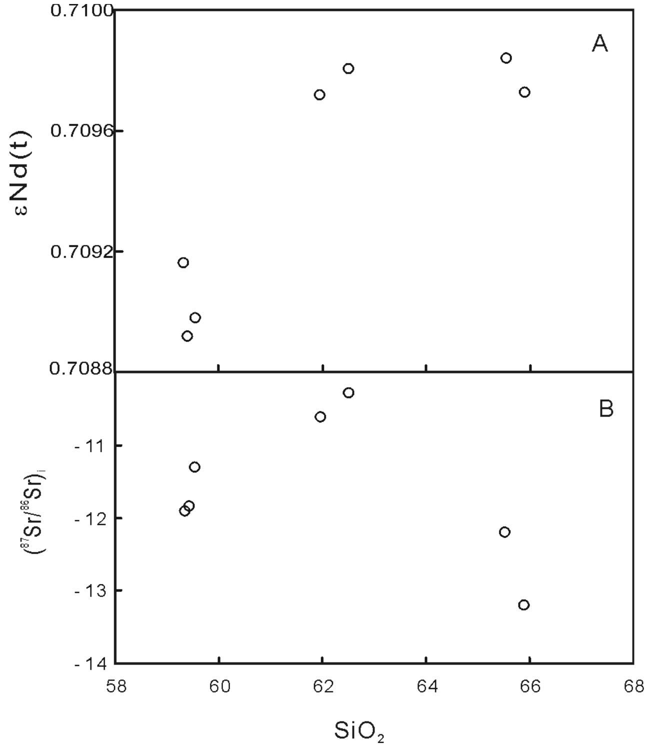

FIG. 9. SiO_2 vs. $\varepsilon_{Nd}(t)$ (A) and ($^{87}Sr/^{86}Sr)_i$ (B) plots of studied adakitic volcanic rocks from Luxi, southeastern NCC.

Yangtze craton crust, which is further supported by the enrichment in incompatible and mobile elements, such as K, Rb, Pb, and the LREEs, and depletion in the HFSEs. However, although the Jurassic–Cretaceous and Cretaceous–Tertiary subduction of the paleo-Pacific plate have been suggested (Chen et al., 2004), there has no evidence up to now suggesting contributions of oceanic crust + sediments to the Mesozoic magmatic activities of the NCC (Zhang et al., 2005b).

Accordingly, we propose a different effect of the Triassic collision between the North China craton and the Yangtze block on the petrogenesis of the adakitic rocks. As a consequence of subduction, the continental crust was compressed and overthickened; the increase in pressure and temperature might have transformed the basaltic lower crust into garnet amphibolite and/or eclogite in the thickened crust region (Austrheim et al., 1997). Basaltic eclogite forms by high- to ultrahigh-pressure metamorphism of basaltic and has a density that is higher than that of lithospheric mantle peridotite by 0.2–0.4g cm^{-3} (Rudnick and Fountain, 1995). The high density thus results in delamination or foundering (Kay and Kay, 1993; Gao et al., 2004) (Fig. 10). Delaminated lower crust inevitably would drag neighboring asthenospheric material along, which must be counterbalanced by a focused, upward-directed return flow (Tilmann et al., 2003). Such an upward heat flow would provide a mechanism for heating the lithospheric mantle, delaminated crust and gradual erosion of remaining crust beneath Luxi. Furthermore, after collision and subduction, the release of stress led to lithospheric extension beneath Luxi. In other words, lithospheric extension might have resulted in the upwelling of the heat flux from the underlying hotter asthenospheric mantle, reheating both lithospheric mantle and source (delaminated lower crust) of the adakitic volcanic rocks. Afterward, dehydration partial melting of the lithospheric mantle and delaminated lower crust (amphibole-bearing eclogite) was triggered. Evidence for this process in Luxi includes post-collision magmatism such as widespread mafic

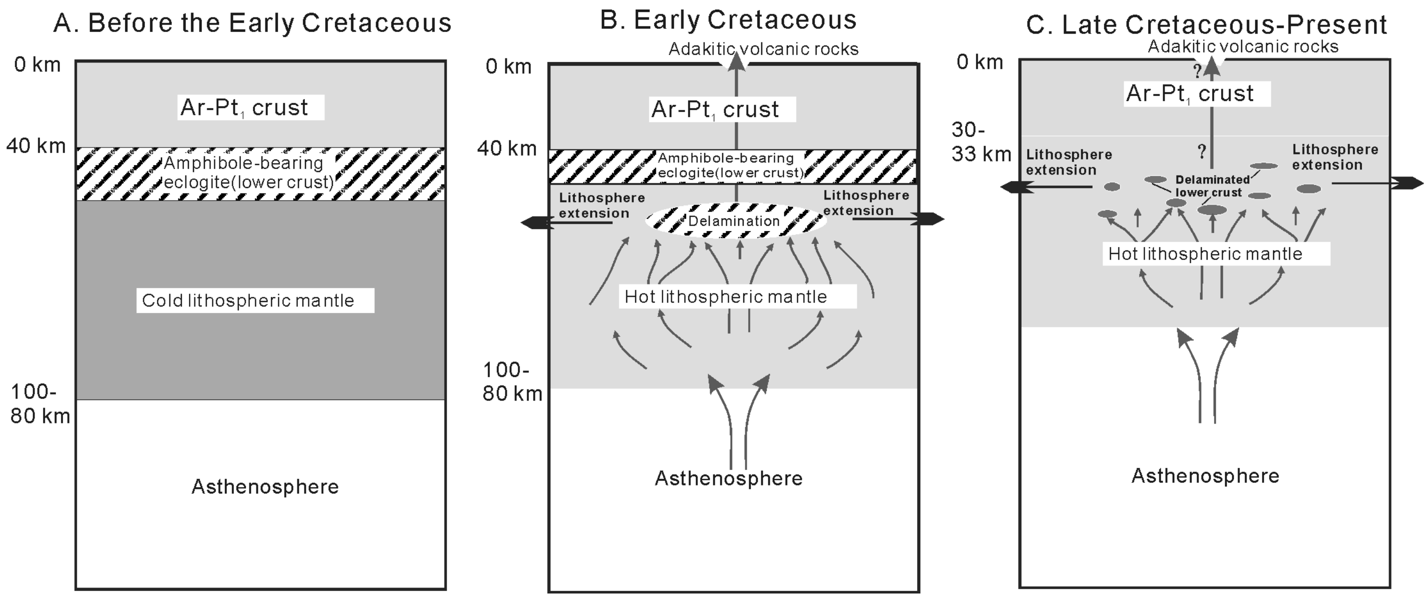

FIG. 10. Model showing that the adakitic volcanic rocks in Luxi resulted from partial melting of delaminated lower crust in the Early Cretaceous. A. Cross-section showing the relatively cold lithospheric mantle and thick crust before the Early Cretaceous. The thick lower crust is composed of amphibole-bearing eclogite. B. The thick lower crust was removed through delamination or foundering due to density instability and sank into the underlying, hot lithospheric mantle. At the same time, hot asthenospheric mantle upwelled due to delamination and lithosphere extension. Adakitic melts were produced by partial melting of the delaminated lower crust, which were heated by the flux of hot lithospheric mantle and upwelling asthenosphere. The adakitic melts reacted with the surrounding mantle peridotite, enhancing their MgO, Cr, and Ni contents. C. Combined lower crustal delamination, surface erosion, and lithospheric or crustal extension led to the present-day thinned crust (30–33 km) (Shi et al., 1989).

dikes (Liu et al., 2004, 2006), alkaline intrusions (Zhang et al., 2005a), and the voluminous volcanic rocks of the Qingshan Formation (Guo, 1999; Qiu et al., 2002) in Luxi. The resulting magmas from melting of delaminated lower crust then reacted with the surrounding mantle peridotite, and formed the Luxi adakitic volcanic rocks with relatively high MgO, Cr, and Ni contents (Fig. 10B and Table 2). Moreover, this process may have culminated in the Late Cretaceous (Fig. 10C).

Dynamic implications

This study provides additional evidence for the recycling of lower continental crust in the NCC, and further support that the foundering was protracted (lasting into the Early Cretaceous before 120 Ma). Dynamic models suggest that delamination of the lower crust probably was accompanied by lithospheric thinning (Jull and Kelemen, 2001). Previous studies indicate that thinned lithosphere existed beneath the eastern NCC (Menzies et al., 1993; Griffin et al., 1998; Gao et al., 2002; Wilde et al., 2003), and this most likely occurred between the Late Jurassic and the Early Cretaceous. The adakitic rocks are characterized by high Sr/Y and La/Yb ratios, indicating the residual presence of garnets and the loss of plagioclase in the source rocks during partial melting. Because such a source is generally thought to have occurred at at a depth of 40 km (1.2 GPa) (Rapp and Watson, 1995; Petford and Atherton, 1996), the Luxi crust was at least that thick when the adakitic magma was produced in the Early Cretaceous. However, the present crustal thickness in the Luxi area is only 30–33 km (Shi et al., 1989). These data imply that the Mesozoic continental crust in the Luxi area was thicker (40 km) than the present crust, and the Luxi crust therefore has most likely undergone a ~10 km thinning process since the late Mesozoic.

However, it is unclear what triggered the density instability and foundering. Based on the investigations of the characteristics of lithospheric mantle beneath the southeastern NCC (including Luxi), Zhang et al. (2005b) proposed that lithospheric thinning was a consequence of interaction between the NCC and the peripheral blocks during the Jurassic–Cretaceous, possibly due to: (1) Jurassic–Cretaceous subduction of the paleo-Pacific (Izanagi) plate (Engebreson et al., 1985), (2) collision of the North China–Mongolian plate with the Siberian plate during closure of a Mongolo-Okhotsk ocean (Davis et al., 2001); and (3) especially the collision of the NCC with the Yangtze block after the closure of a paleo-Tethyan ocean during the Triassic (240–220 Ma). Similar mechanisms except for (3) triggering density instability and foundering of the NCC lower continental crust have been proposed (Gao et al., 2004). Nevertheless, on the basis of the geochemical features and ages of the adakitic rocks in Luxi, we suggest that the most likely mechanism inducing lithospheric thinning beneath Luxi may have been the Triassic collision between the NCC and the Yangtze block.

Conclusions

The newly analyzed 116–120 Ma volcanic rocks at Luxi have adakitic geochemical affinities. These rocks were derived from melting of delaminated lower crust, triggered by heat flux from the underlying mantle or asthenosphere, leaving a residual garnet ± amphibole–bearing protolith. Their relatively high MgO, Cr, and Ni contents indicate that the adakitic rocks contain a significant mantle component due to interaction between the ascending magmas and the surrounding mantle peridotite. This study provides further evidence for the foundering of lower continental crust in the NCC.

Acknowledgments

This research was supported by the Chinese 973 program (2007CB411402), the Knowledge Innovation project (KZCX2-YW-111-03), National 305 project (2006BAB07B04-04), and the National Nature Science Foundation of China (40673029, 40773020, 90714010, and 40634020). Pang Kwan-Nang is thanked for a helpful review of a previous version of the manuscript. We are grateful to Zhu-Ying Chu, and Chao-Feng Li for Sr and Nd isotopic analyses. Thanks also are due to the Shandong Provincial Department of Land and Resources for providing regional geologic data.

REFERENCES

Aguillo'n-Robles, A., Caimus, T., Bellon, H., Maury, R. C., Cotton, J., Bourgois, J., and Michaud, F., 2001, Late Miocene adakites and Nb-enriched basalts from Vizcaino Peninsula, Mexico: Indicators of East Pacific Rise subduction below southern Baja California: Geology, v. 29, p. 531–534.

Atherton, M. P., and Petford, N., 1993, Generation of sodium-rich magmas from newly underplated basaltic crust: Nature, v. 362, p. 144–146.

Austrheim, H., Eramber, M., and Engvik, A. K., 1997, Processing of crust in the root of the Caledonian continental collision zone: The role of eclogitization: Tectonophysics, v. 273, p. 121–153.

Baker, M. B., Hischmann, M. M., Ghiorso, M. S., and Stolper, E. M., 1995, Compositions of near-solidus peridotite melt from experiments and thermodynamic calculations: Nature, v. 375, p. 308–311.

Chen, B., Jahn, B. M., Arakawa, A., and Zhai, M. G., 2004, Petrogenesis of the Mesozoic intrusive complexes from the southern Taihang Orogen, North China craton and Sr-Nd- Pb isotopic constraints: Contributions to Mineralogy and Petrology, v. 148, p. 489–501.

Castillo, P. R., Janney, P. E., and Solidum, R. U., 1999, Petrology and geochemistry of Camiguin Island, southern Philippines: Insights to the source of adakites and other lavas in a complex arc setting: Contributions to Mineralogy and Petrology, v. 134, p. 33–51.

Davis, G. A., Yadong, Z., Cong, W., Darby, B. J., Changhou, Z., and Gehrels, G., 2001, Mesozoic tectonic evolution of the Yanshan fold and thrust belt, with emphasis on Hebei and Liaoning provinces, northern China, *in* Hendrix, M. S., and Davis, G. A., eds., Paleozoic and Mesozoic tectonic evolution of Central Asia: From continental assembly to intracontinental deformation: Boulder, CO, Geological Society of America, Memoir 194, p. 171–197.

Defant, M. J., and Drummond, M. S., 1990, Derivation of some modern arc magmas by melting of young subducted lithosphere: Nature, v. 347, p. 662–665.

Defant, M. J., Jackson, T. E., Drummond, M. S., De Boer, J. Z., Bellon, H., Feigenson, M. D., et al., 1992, The geochemistry of young volcanism throughout western Panama and southeastern Costa Rica: An overview: Journal of the Geological Society, London, v. 149, p. 569–579.

Defant, M. J., and Kapezhinskas, P. K., 2001, Evidence suggests slab melting in arc magmas. EOS (Transactions of the American Geophysical Union), v. 82, p. 65–69.

Defant, M. J., Kepezhinskas, P., Defant, M. J., Xu, J. F., Kepezhinskas, P., Wang, Q., Zhang, Q., and Xiao, L., 2002, Adakites: Some variations on a theme: Acta Petrological Sinica, v. 18, p. 129–142.

Drummond, M. S., Defant, M. J., and Kepezhinskas, P. K., 1996, Petrogenesis of slab-derived trondhjemite-tonalite-dacite/adakite magmas: Transactions of the Royal Society of Edinburgh, Earth Sciences, v. 87, p. 205–215.

Engebreson, D. C., Cox, A., and Gordon, R. G., 1985, Relative motions between oceanic and continental plates in the Pacific basins: Geological Society of America, Special Paper 206, p. 1–59.

Gao, S., Rudnick, R. L., Carlson, R. W., McDonough, W. F., and Liu, Y. S., 2002, Re-Os evidence for replacement of ancient mantle lithosphere beneath the North China Craton: Earth and Planetary Science Letters, v. 98, p. 307–322.

Gao, S., Rudnick, R., Yuan, H. L., Liu, X. M., Liu, Y. S., Xu, W. L., Ling, W. L., Ayers, J., Wang, X. C., and Wang, Q. H., 2004, Recycling lower continental crust in the north China craton: Nature, v. 432, p. 892–897.

Green, T. H., 1980, Island arc and continent-building magmatism: A review of petrogenetic models based on experimental petrology and geochemistry: Tectonophysics, v. 63, p. 367–385.

Griffin, W. L., Zhang, A. D., O'Reilly, S. Y., and Ryan, C. G., 1998, Phanerozoic evolution of the lithosphere beneath the Sino-Korean craton, *in* Flower, M., Chung, S.-L., Lo, C.-H., and Lee, T.-Y., Mantle dynamics and plate interactions in East Asia: Washington DC, American Geophysical Union, Geodynamics Series, no. 27, p. 107–126.

Guo, F., 1999, The petrogenesis of Mesozoic volcanic rocks in Shandong Province, eastern China and their constraints on the lithospheric thinning process: Unpubl. Ph.D. thesis, Institute of Geotectonics, Chinese Academy of Sciences, Changsha (in Chinese).

Guo, F., Fan, W. M., and Li, C .W., 2006, Geochemistry of late Mesozoic adakites from the Sulu belt, eastern China: Magma genesis and implications for crustal recycling beneath continental collisional orogens: Geological Magazine, v. 143, p. 1–13.

Guo, F., Fan, W. M., Wang, Y. J., and Lin, G., 2003, Geochemistry of late Mesozoic mafic magmatism in west Shandong Province, eastern China. Characterizing the lost lithospheric mantle beneath the North China Block: Geochemical Journal, v. 40, p. 63–77.

Jahn, B. M., and Zhang, J. Q., 1984, Archean granulite gneisses from eastern Sino-Korean Province, China: Rare earth geochemistry and tectonic implications: Contributions to Mineralogy and Petrology, v. 85, p. 224–243.

Johnson, K., Barnes, C. G., and Miller, C. A., 1997, Petrology, geochemistry, and genesis of high-Al tonalite and trondhjemites of the Cornucopia stock, Blue Mountains, Northeastern Oregon: Journal of Petrology, v. 38, p. 1585–1611.

Jull, M., and Kelemen, P. B., 2001, On the conditions for lower crustal convective instability: Journal of Geophysical Research, v. 106, p. 6423–6446.

Kay, R. W., 1978, Aleutian magnesian andesites—melts from subducted Pacific ocean crust: Journal of Volcanology and Geothermal Research, v. 4, 117–132.

Kay, R. W., and Kay, S. M., 1991, Creation and destruction of lower continental crust: Geologische Rundschau, v. 80, p. 259–278.

Kay, R. W., and Kay, S. M., 1993, Delamination and delamination magmatism: Tectonophysics, v. 219, p. 177–189.

Kay, S. M., Ramos, V. A., and Marquez, M., 1993, Evidence in Cerro Pampa volcanic rocks of slab melting prior to ridge trench collision in southern South America: Journal of Geology, v. 101, p. 703–714.

Kepezhinskas, P. K., Defant, M. J., and Drummond, M., 1995, Na metasomatism in the island-arc mantle by slab melt–peridotite interaction: Evidence from mantle interaction—evidence from mantle xenoliths in the north Kamchatka arc: Journal of Petrology, v. 36, p. 1505–1527.

Le Bas, M. J., Le Maitre, R. W., Streckeisen, A., and Zanettin, B., 1986, A chemical classification of volcanic rocks based on the total alkali-silica diagram: Journal of Petrology, v. 27, p. 745–750.

Liu, S., Hu, R. Z., Zhao, J. H., and Feng, C. X., 2004, K-Ar geochronology of Mesozoic mafic dikes in Shandong Province, eastern China: Implications for crustal extension: Acta Geologica Sinica, v. 78, p. 1207–1213.

Liu, S., Zou, H. B., Hu, R. Z., Zhao, J. H., and Feng, C. X., 2006, Mesozoic mafic dikes from the Shandong Peninsula, North China craton: Petrogenesis and tectonic implications: Geochemical Journal, v. 40, p. 181–195.

Lugmair, G. W., and Harti, K., 1978, Lunar initial $^{143}Nd/^{144}Nd$: Differential evolution of the lunar crust and mantle: Earth and Planetary Science Letters, v. 39, p. 349–357.

Macpherson, C. G., Dreher, S. T., and Thirlwall, M. F., 2006, Adakites without slab melting: High pressure differentiation of island arc magma, Mindanao, the Philippines. Earth and Planetary Science Letters, v. 243, p. 581–593.

Mahoney J. J., Frei, R., Tejada, M. L. G., Mo, X. X., and Leat, P. T., 1998, Tracing the Indian Ocean mantle domain through time: Isotopic results from old West Indian, East Tethyan and South Pacific seafloor: Journal of Petrology, v. 39, p. 1285–1306.

Martin, H., 1998, Adakitic magmas: Modern analogues of Archaean granitoids: Lithos, v. 46, p. 411–429.

Martin, H., Smithies, R. H., Rapp, R., Moyen, J. F., and Champion, D., 2005, An overview of adakite, tonalite–trondhjemite–granodiorite (TTG), and sanukitoid: Relationships and some implications for crustal evolution: Lithos, v. 79, p. 1–24.

Menzies, A., Fan, W.-M., and Zhang, M., 1993, Palaeozoic and Cenozoic lithoprobes and loss of >120 km of Archean lithosphere, Sino-Korean craton, China, *in* Prichard, H. M., Alabaster, H. M., Harris, T., and Neary, C. R., eds., Magmatic processes and plate Tectonics, Geological Society, London, Special Publications, v. 76, p. 71–81.

Muir, R. J., Weaver, S. D., Bradshaw, J. D., Eby, G. N., and Evans, J. A., 1995, Geochemistry of the Cretaceous Separation Point Batholith, New Zealand: Granitoid magmas formed by melting of mafic lithosphere: Journal of the Geological Society, London, v. 152, p. 689–701.

Pearce, J. A., and Norry, M. J., 1979, Petrogenetic implications of Ti, Zr, Y, and Nb variations in volcanic rocks. Contributions to Mineralogy and Petrology, v. 69, p. 33–47.

Petford, N., and Atherton, M., 1996, Na-rich partial melts from newly underplated basaltic crust: The Cordillera Blanca Batholith, Peru: Journal of Petrology, v. 37, p. 1491–1521.

Qi, L., Hu, J., and Grégoire, D. C., 2000, Determination of trace elements in granites by inductively coupled plasma mass spectrometry: Talanta, v. 51, p. 507–513.

Qiu, J. S., Xu, X. S., and Luo, Q. H., 2001, Potassic lavas and lamprophyre in western Shangdong: ^{40}Ar-^{39}Ar dating and petrogenesis: Chinese Science Bulletin, v. 46, p. 1500–1508.

Qiu, J. S., Xu, X. S., and Luo, Q. H., 2002, Potassium-rich volcanic rocks and lamprophyres in western Shandong Province: ^{40}Ar–^{39}Ar dating and source tracing: Chinese Science Bulletin, v. 47, p. 91–99.

Rapp, R. P., Shimizu, N., and Norman, M. D., 2003, Growth of early continental crust by partial melting of eclogite: Nature, v. 425, p. 605–609.

Rapp, R. P., Shimizu, N., Norman, M. D., and Applegate, G. S., 1999, Reaction between slab-derived melts and peridotite in the mantle wedge: Experimental constraints at 3.8 GPa: Chemical Geology, v. 60, p. 335–356.

Rapp, R. P., and Watson, E. B., 1995, Dehydration melting of metabasalt at 8–32 kbar: Implications for continental growth and crust-mantle recycling: Journal of Petrology, v. 36, p. 891–931.

Rapp, R. P., Watson, E. B., and Miller, C. F., 1991, Partial melting of amphibolite/eclogite and the origin of Archean trondhjemites and tonalites: Precambrian Research, v. 51, p. 1–25.

Rudnick, R. L., 1995, Making continental crust: Nature, v. 378, p. 571–578.

Rudnick, R. L., and Fountain, D. M., 1995, Nature and composition of the continental crust: A lower crustal perspective: Reviews in Geophysics, v. 33, p. 267–309.

Sajona, F. G., Naury, R. C., Pubellire, M., Leterrier, J., Bellon, H., and Cotton, J., 2000, Magmatic source enrichment by slab-derived melts in young post-collision setting, central Mindanao (Philippines): Lithos, v. 54, p. 173–206.

Shi, Z. H., Liu, Z. P., and Yin, X. H., 1989, Crust thickness (calculated by gravity), *in* Ma, X. Y., ed.-in-chief, Lithosphere dynamics atlas of China: Beijing, China, Seismological Publishing House.

Smithies, R. H., 2000, The Archaean tonalite-trondhjemite-granodiorite (TTG) series is not an analogue of Cenozoic adakite: Earth and Planetary Science Letters, v. 182, p. 115–125.

Song, M. C., and Li, H. K., 2001, Study on regional geological structural evolution in Shandong Province: Shandong Geology, v. 17, p. 11–21 (in Chinese).

Steiger, R. H., and Jäger, E., 1977, Subcommission on Geochronology; convention on the use of decay constants in geochronology and cosmochronology: Earth and Planetary Science Letters, v. 36, p. 359–362.

Stern, C. R., and Kilian, R., 1996, Role of the subducted slab, mantle wedge, and continental crust in the generation of adakites from the Austral volcanic zone: Contributions to Mineralogy and Petrology, v. 123, p. 263–281.

Stern, R. A., and Hanson, G. N., 1991, Archean high-Mg granodiorite: A derivative of light rare earth element–enriched monzodiorite of mantle origin, Journal of Petrology, v. 32, p. 201–238.

Sun, S. S., and McDonough, W. F., 1989, Chemical and isotopic systematics of oceanic basalts: Implications for mantle composition and processes, *in* Saunders, A. D., and Norry, M. J., eds., Magmatism in the ocean basins: Geological Society, London, Special Publication, v. 42, p. 313–345.

Tan, D., and Lin, J., 1994, Mesozoic potassic magma province on North China platform: Beijing, China, Seismological Press, 184 p. (in Chinese).

Tatsumi, Y., 1986, Chemical characteristics of fluid phase released from a subduction lithosphere and origin of arc magma: Evidence from high-pressure experiments and natural rocks: Journal of Volcanology and Geothermal Research, v. 29, p. p. 293–309.

Tilmann, F., Ni, J., and I. I. S. Team, 2003, Seismic imaging of the downwelling Indian lithosphere beneath central Tibet: Science, v. 300, p. 1424–1427.

Tribuzio, R., Thirlwall, M. F., Vannucci, R., and Matthew, F., 2004, Origin of the gabbro-peridotite association from the Northern Apennine ophiolites, Italy: Journal of Petrology, v. 45, p. 1109–1124.

Wang, Q., 2000, Study pertaining to rock probes of the dynamics of the deep Earth: Examples of adakitic and alkali-rich igneous rocks in Southeast China (including the Dabie Orogen): Postdoctoral research report, Guanzhou Institute of Geochemistry, Chinese Academy of Sciences, p. 69–108 (in Chinese with English abstract).

Wang, Q., Xu, J. F., Jian, P., Bao, Z. W., Zhao, Z. H., Li, C. F., Xiong, X. L., and Ma, J. L., 2006, Petrogenesis of adakitic porphyries in an extensional tectonic setting, Dexing, South China: Implications for the genesis of porphyry copper mineralization: Journal of Petrology, v. 47, p. 119–147.

Wang, Q., Xu, J. F., Zhao, Z. H., Bao, Z. W., Xu, W., and Xiong, X. L., 2004, Cretaceous high-potassium intrusive rocks in the Yueshan–Hongzhen area of east China: Adakites in an extensional tectonic regime within a continent: Geochemical Journal, v. 38, p. 417–434.

Wang, Q., Xu, J. F., Zhao, Z. H., Xiong, X. L., and Bao, Z. W., 2003a, Petrogenesis of the Mesozoic intrusive rocks in the Tongling area, Anhui Province, China and their constraint to geodynamic processes: Science in China, Series D, v. 46, p. 801–815.

Wang, Q., Zhao, Z. H., Xu, J. F., Li, X. H., Bao, Z. W., and Xiong X. L., 2003b, Petrogenesis and metallogenesis of the Yanshanian adakite-like rocks in the Eastern Yangtze Block: Science in China, Series D, v. 46 (suppl.), p. 164–176.

Wilde, S. A., Zhou, X. H., Nemchin, A. A., and Sun, M., 2003, Mesozoic crust-mantle interaction beneath the North China craton: A consequence of the dispersal of Gondwanaland and accretion of Asia: Geology, v. 31, p. 817–820.

Xiong, X. L., Li, X. H., Xu, J. F., Li, W. X., Zhao Z. H., and Wang, Q., 2003, Extremely high-Na adakite-like magmas derived from alkali-rich basaltic underplate: The Late Cretaceous Zhantang andesites in the Huichang Basin, SE China: Geochemical Journal, v. 37, p. 233–252.

Xu, J. F., and Castillo, P. R., 2004, Geochemical and Nd–Pb isotopic characteristics of the Tethyan asthenosphere: Implications for the origin of the Indian Ocean mantle domain: Tectonophysics, v. 393, p. 9–27.

Xu, J. F., Castillo, P. R., Chen, F. R., Niu, H. C., Yu, X. Y., and Zhen, Z. P., 2003, Geochemistry of late Paleozoic mafic igneous rocks from the Kuerti area, Xinjiang, northwest China: Implications for backarc mantle evolution: Chemical Geology, v. 193, p. 137–154.

Xu, J. F., Shinjo, R., Defant, M. J., Wang, Q. A., and Rapp, R. P., 2002, Origin of Mesozoic adakitic intrusive rocks in the Ningzhen area of east China: Partial melting of delaminated lower continental crust?: Geology, v. 30, p. 1111–1114.

Xu, W. L., Chi, X. G., Yuan, C., and Wang, W., 1993, Mesozoic dioritic rocks and deep-seated inclusions in the central North China Platform: Beijing, China, Geological Publishing House, 164 p. (in Chinese).

Xu, W. L., Wang, D. Y., Wang, Q. H., Pei, F., and Lin, J. Q., 2004a, $^{40}Ar/^{39}Ar$ dating of hornblende and biotite in Mesozoic intrusive complex from the North China Block: Constraints on the time of lithospheric thinning: Geochimica, v. 33, p. 221–231 (in Chinese).

Xu, Y. G., 2002, Evidence for crustal components in mantle source and constraints on recycling mechanism: Pyroxenite xenoliths from Hannuoba, North China: Chemical Geology, v. 182, p. 301–322.

Xu, Y. G., Huang, X. L., Ma, J. L., Wang, Y. B., Lizuka, Y., Xu, J. F., Wang, Q. and Wu, X. Y., 2004b, Crust-mantle interaction during the tectono-thermal reactivation of the North China craton: Constraints from SHRIMP zircon U-Pb chronology and geochemistry of Mesozoic plutons from western Shandong: Contributions to Mineralogy and Petrology, v. 147, p. 750–767.

Xu, Y. G., Ma, J. L., Huang, X. L., Lizuka, Y., Chung, S. L., Wang, Y. B., and Wu, X. Y., 2004b, Early Cretaceous gabbroic complex from Yinan, Shandong Province: Petrogenesis and mantle domains beneath the North China craton: International Journal of Earth Science, v. 93, p. 1025–1041.

Zhang, H. F., and Sun, M., 2002, Geochemistry of Mesozoic basalts and mafic dikes in southeastern North China craton, and tectonic implications: International Geology Review, v. 44, p. 370–382.

Zhang, H. F., Sun, M., Zhou, X. H., Fan, W. M., Zhai, M. G., and Yin, J. F., 2002, Mesozoic lithosphere destruction beneath the North China Craton: Evidence from major-, trace element, and Sr-Nd-Pb isotope studies of Fangcheng basalts: Contributions to Mineralogy and Petrology, v. 144, p. 241–253.

Zhang, H. F., Sun, M., Zhou, M. F., Fan, W. M., Zhou, X. H., and Zhai, M. G., 2004, Highly heterogeneous Late Mesozoic lithospheric mantle beneath the North China Craton: Evidence from Sr–Nd–Pb isotopic systematics of mafic igneous rocks: Geological Magazine, v. 41, p. 55–62.

Zhang, H. F., Sun, M., Zhou, X. H., and Ying, J. F., 2005a, Geochemical constraints on the origin of Mesozoic alkaline intrusive complexes from the North China craton and tectonic implications: Lithos, v. 81, p. 297–317.

Zhang, H. F., Zhou, X. H., Fan, W. M., Sun, M., Guo, F., Ying, J. F., Tang, Y. J., Zhang, J., and Niu, L. F., 2005b, Nature, composition, enrichment processes and its mechanism of the Mesozoic lithospheric mantle beneath the southeastern North China craton: Acta Petrologica Sinica, v. 21, p. 1271–1280 (in Chinese).